Front. Phys. 10(5), 100306 (2015)
DOI 10.1007/s11467-015-0505-x

RESEARCH ARTICLE

# Trapped Bose–Einstein condensates in synthetic magnetic field

**Qiang Zhao**[1,2], **Qiang Gu**[1,†]

[1] *Department of Physics, University of Science and Technology Beijing, Beijing 100083, China*
[2] *School of Science, North China University of Science and Technology, Tangshan 063009, China*
*Corresponding author. E-mail:* [†] *qgu@ustb.edu.cn*
*Received May 17, 2015; accepted July 2, 2015*

The rotational properties of Bose–Einstein condensates in a synthetic magnetic field are studied by numerically solving the Gross–Pitaevskii equation and comparing the results to those of condensates confined in a rotating trap. It appears to be more difficult to add a large angular momentum to condensates spun up by the synthetic magnetic field than by the rotating trap. However, strengthening the repulsive interaction between atoms is an effective and realizable route to overcoming this problem and can at least generate vortex-lattice-like structures. In addition, the validity of the Feynman rule for condensates in the synthetic magnetic field is verified.

**Keywords** Bose–Einstein condensates, synthetic magnetic field, vortices

**PACS numbers** 03.75.Lm, 03.75.Hh, 05.30.Jp



## 1 Introduction

Rotating quantum gas has attracted enormous research interest because it exhibits a number of counterintuitive phenomena unlike those of classical gas. One of its striking features is that vortices inside it are quantized. This feature has been extensively explored in the context of superfluid $^4$He [1] and $^3$He [2, 3], and superconductors [4]. The recent realization of atomic Bose–Einstein condensates (BECs) opens up a new avenue toward understanding the physics of rotating quantum gases [5]. The atomic BEC has advantages over superfluid $^4$He and $^3$He because it is flexibly manipulated and can be easily rotated using several techniques.

The first reported vortex in BECs was created by a phase engineering technique using laser beams in which a binary mixture of condensates was manipulated, and quantized rotation of one component was realized [6]. Soon after, the rotating frame method succeeded in experiments in which the condensate was spun up by rotational deformation of a confining trap [7]. This approach is similar to the rotating-bucket method in experimental studies of superfluid $^4$He [1]. One quantized vortex appeared as the rotational frequency rose to a certain critical value for the deformed trap [7, 8]. With increasing rotational frequency, the number of vortices increased. Vortex lattices [9–11] were also obtained at higher rotational frequencies. Further increasing the rotational frequency drove the condensates to a fast rotation regime [12, 13].

The angular momentum of a rotating classical fluid is proportional to its rotational frequency. For a quantum gas, the angular momentum is characterized by the total number of vortices it carries. The relation between the number of vortices and the rotational frequency is described by the well-known Feynman rule [14], which can be expressed as $2\pi\hbar N_V/m = 2\Omega A$, where $\Omega$ is the rotational frequency, and $N_V$ is the vortex number within area $A$. The Feynman rule was deduced originally for superfluid helium in a rotating bucket. In view of the analogy between the rotating bucket and the rotating trap, the Feynman rule is naturally applicable to atomic BECs in the rotating trap. The validity of the Feynman rule has been intensively studied both theoretically [15–17] and experimentally [10, 18] in recent years.

The rotating frame approach is subject to some limitations; e.g., it is difficult to add optical lattices, and the rotation is limited by the heating, metastability, and so on. The synthetic magnetic field approach stands out and is expected to overcome the above limitations [19, 20]. This novel approach creates a vector potential for atoms by dressing them in a space-dependent manner with an optical field and thus makes neutral atoms behave like charged particles in a magnetic field [19]. Vortices were observed experimentally in a condensate for a synthetic magnetic field greater than the critical value [20]. The hydrodynamical behavior of a condensate in a synthetic

magnetic field and the dynamical instability of vortex nucleation were studied in Ref. [21]. Enormous effort was devoted to studying cold atoms subject to a synthetic magnetic field in the presence of optical lattices. Experimentally, a synthetic magnetic field has been engineered in periodic lattices [22]. Theoretically, the Berezinskii–Kosterlitz–Thouless transition in a two-dimensional (2D) lattice has been investigated [23, 24], and the Hofstadter butterfly physics in a strong field has been discussed [25, 26].

The thermodynamic properties of an ideal Bose gas in a synthetic magnetic field have also been studied [27, 28]. It is natural to expect that rotating the gas decreases the Bose–Einstein condensation temperature. These studies [27, 28] show that Bose–Einstein condensation can be more easily suppressed in a rotating frame than in a synthetic magnetic field, which implies that a rotating frame can spin up the atomic gas more efficiently than a synthetic magnetic field. If this is true, it is more difficult to add a large angular momentum to condensates using a synthetic magnetic field than it is using a rotating frame. Therefore, it is worthwhile to check this issue carefully and to thoroughly compare the two approaches.

In this paper, we focus on the rotational properties of atomic BECs in a synthetic magnetic field. Vortex formation is investigated by numerically solving the Gross–Pitaevskii (GP) equation, with an emphasis on the difference between the results for a synthetic magnetic field and for a rotating frame. This paper is organized as follows. Section 2 introduces the GP equations of BECs in both a magnetic field and a rotating frame. Section 3 presents the numerical results and discusses the difference between the two approaches. A brief conclusion is given in Section 4.

## 2 The model

The effective Hamiltonian for a neutral atom of mass $m$ in a synthetic magnetic field is given by

$$H = \frac{1}{2m}(\boldsymbol{P}-\boldsymbol{A})^2 + \frac{1}{2}m\omega_0^2(x^2+y^2) + \frac{1}{2}m\omega_z^2 z^2, \quad (1)$$

where $\boldsymbol{P}$ is the canonical momentum operator, and $\boldsymbol{A}$ is the synthetic gauge potential. Here the atomic BEC is confined in an anisotropic harmonic trap, and $\omega_0$ and $\omega_z$ are the trap frequencies in the $x$–$y$ plane and on the $z$ axis, respectively. We assume that the synthetic field $\boldsymbol{B} = 2m\Omega\vec{e}_z$ is parallel to the $z$ axis and choose the symmetric gauge $\boldsymbol{A} = (\boldsymbol{B}\times\boldsymbol{r})/2 = m(\boldsymbol{\Omega}\times\boldsymbol{r})$, where $\Omega$ is the Larmor frequency. Therefore, the GP equation for BEC can be written as

$$\mathrm{i}\hbar\frac{\partial\psi(\boldsymbol{r},t)}{\partial t} = \left[\frac{1}{2m}(\boldsymbol{P}-\boldsymbol{A})^2 + V'(\boldsymbol{r}) + g|\psi|^2\right]\psi(\boldsymbol{r},t), \quad (2)$$

where $V'(\boldsymbol{r}) = \frac{1}{2}m\omega_0^2(x^2+y^2) + \frac{1}{2}m\omega_z^2 z^2$, $\psi(\boldsymbol{r},t)$ is the wave function of the condensates, and $g = 4\pi\hbar^2 a_s/m$ is the contact interaction strength between atoms with s-wave scattering length $a_s$. In this work, we consider pancake-shaped BECs; that is, the harmonic trapping frequencies satisfy $\omega_z \gg \omega_0$.

For convenience, Eq. (2) can be expressed using dimensionless quantities, where the spatial coordinates $x$, $y$, and $z$ are normalized by the characteristic harmonic oscillator length $a_0 = \sqrt{\hbar/(m\omega)}$ with $\omega = \min\{\omega_0,\omega_z\} = \omega_0$, and the time $t$ is in units of $\omega_0^{-1}$. Then Eq. (2) is reduced to the dimensionless form

$$\mathrm{i}\frac{\partial\tilde{\psi}(\tilde{\boldsymbol{r}},\tilde{t})}{\partial\tilde{t}} = \left[\frac{1}{2}(\tilde{\boldsymbol{P}}-\tilde{\boldsymbol{A}})^2 + V(\tilde{\boldsymbol{r}}) + \beta|\tilde{\psi}|^2\right]\tilde{\psi}(\tilde{\boldsymbol{r}},\tilde{t}), \quad (3)$$

where $V(\tilde{\boldsymbol{r}}) = \frac{1}{2}\gamma_0^2(\tilde{x}^2+\tilde{y}^2) + \frac{1}{2}\gamma_z^2\tilde{z}^2$, $\gamma_0 = \omega_0/\omega = 1$, $\gamma_z = \omega_z/\omega_0$, and $\beta = 4\pi N a_s/a_0$. Here, dimensionless variables are denoted with a tilde. Because of $\omega_z \gg \omega_0$, the wave function can be supposed to be in a separated variables form,

$$\tilde{\psi}(\tilde{\boldsymbol{r}},\tilde{t}) = \tilde{\psi}_{2\mathrm{D}}(\tilde{x},\tilde{y},\tilde{t})\tilde{\psi}_{1\mathrm{D}}(\tilde{z})\mathrm{e}^{-\mathrm{i}\gamma_z\tilde{t}/2},$$

where

$$\tilde{\psi}_{1\mathrm{D}}(\tilde{z}) = (\gamma_z/\pi)^{1/4}\mathrm{e}^{-\gamma_z\tilde{z}^2/2}$$

is the ground state of the harmonic oscillator along the $z$ direction. After integrating out the coordinate $z$, we obtain the 2D GP equation,

$$\mathrm{i}\frac{\partial\tilde{\psi}_{2\mathrm{D}}(\tilde{x},\tilde{y},\tilde{t})}{\partial\tilde{t}} = \left[\frac{1}{2}(\tilde{\boldsymbol{P}}-\tilde{\boldsymbol{A}})^2 + \frac{1}{2}(\tilde{x}^2+\tilde{y}^2) + g_{2\mathrm{D}}|\tilde{\psi}_{2\mathrm{D}}|^2\right]\tilde{\psi}_{2\mathrm{D}}(\tilde{x},\tilde{y},\tilde{t}), \quad (4)$$

where $g_{2\mathrm{D}} = \beta\sqrt{\gamma_z/2\pi}$ represents the effective 2D interaction strength. We note that $\gamma_z$ is just the trap aspect ratio of the anisotropic trap.

For comparison, we also consider the properties of BECs in a rotating frame. In this case, the single-particle Hamiltonian is given by

$$H = \frac{1}{2m}(\boldsymbol{P}-\boldsymbol{A})^2 + \frac{m}{2}(\omega_0^2-\Omega^2)(x^2+y^2) + \frac{m}{2}\omega_z^2 z^2. \quad (5)$$

Here $\boldsymbol{A} = m(\boldsymbol{\Omega}\times\boldsymbol{r})$, and $\Omega$ denotes the rotational frequency of the trap, which is comparable to the Larmor frequency in Eq. (1). Therefore, both of them are referred to as the rotational frequency in this paper. Using the same procedure, we obtain the corresponding 2D GP equation in the dimensionless form:

$$\mathrm{i}\frac{\partial\tilde{\psi}_{2\mathrm{D}}(\tilde{x},\tilde{y},\tilde{t})}{\partial\tilde{t}} = \left[\frac{1}{2}(\tilde{\boldsymbol{P}}-\tilde{\boldsymbol{A}})^2+\frac{1}{2}(1-\frac{\Omega^2}{\omega_0^2})(\tilde{x}^2+\tilde{y}^2) + g_{2\mathrm{D}}|\tilde{\psi}_{2\mathrm{D}}|^2\right]\tilde{\psi}_{2\mathrm{D}}(\tilde{x},\tilde{y},\tilde{t}). \quad (6)$$

In our calculation, we use the Fourier spectral method to solve the nonlinear differential equations (4) and (6) via the imaginary time propagation approach [29]. Although these two equations do not differ fundamentally, the comparison indicates apparently different physical behavior. The calculation starts with some initial states and then propagates until numerical convergence is achieved.

## 3 Results and discussion

The GP equation provides a remarkably reliable description of the physics of an atomic condensate. The properties of atomic BECs in a rotating frame have been intensively investigated using the GP equation [15–17]. Vortex formation has been discussed in detail in terms of the rotational frequency, the contact interaction between atoms, and the aspect ratio of the traps. Hereinafter, the corresponding results for BECs in a synthetic magnetic field are examined. The focus is on the difference between the two cases.

### 3.1 Effect of the rotational frequency on vortex formation

The formation of quantum vortices and the dependence of the vortex number on the rotational frequency are among the most important issues for rotating quantum gases. Unlike the classical case, no angular momentum can be added to the quantum gas until the rotational frequency exceeds a critical value, at which one quantized vortex begins to form. Then more vortices appear as the rotational frequency increases further.

Figure 1 shows the 2D atom density at different rotational frequencies for BECs with the dimensionless contact interaction $g_{2\mathrm{D}} = 100$ in the rotating frame and synthetic magnetic field. The critical rotational frequencies for creation of the first vortex inside the BECs in the rotating frame and synthetic magnetic field are $0.369\omega_0$ and $0.388\omega_0$, respectively. The two values are very similar, and the latter is slightly larger than the former.

However, the two types of rotation exhibit a remarkable difference at high rotational frequency. For BECs in the rotating frame, the vortex number grows quickly with $\Omega$, especially when $\Omega$ approaches the trapping frequency $\omega_0$. For example, there are about 10 vortices at $\Omega/\omega_0 = 0.95$, and the vortex number is 56 at $\Omega = 0.99\omega_0$, which is just the upper limit of the rotational frequency. Moreover, the BEC expands significantly. It can be seen that the condensate occupies almost the entire square region under consideration in our calculation when $\Omega$ rises to $0.99\omega_0$. The vortex structure resembles the Abrikosov vortex lattice. We note that the obtained results may not be sufficiently accurate when $\Omega$ is close to $\omega_0$, because the boundary condition we choose in the calculation may not be well met.

For the BECs rotated by the synthetic magnetic field, the vortex number obviously grows much more slowly. After one vortex is created, the vortex number remains unchanged even when $\Omega$ reaches $0.8\omega_0$. It seems rather difficult to add more vortices. Only 4 vortices emerge at $\Omega = 0.99\omega_0$. The Larmor frequency can be larger than $\omega_0$. Actually, there is no intrinsic upper limit value for $\Omega$, which depends only on the strength of the synthetic magnetic field. Figure 1 shows the results for $\Omega > \omega_0$. The vortex number rises, but still slowly. There are about 12 vortices at $\Omega = 1.9\omega_0$. This number is still small. In experiments, about 10 vortices were observed in BECs under a synthetic field [19, 20].

Another difference from the rotating frame case is that the size of the condensates remains almost unchanged as $\Omega$ increases. This point is clearly shown in Fig. 1.

The above results indicate that it is hard to create vortices in BECs rotated by the synthetic magnetic field, as suggested by thermodynamic calculations [27, 28]. To illustrate this point further, we calculate the critical rotational frequencies, $\Omega_c/\omega_0$, for creating a certain number of vortices, $N_V$, for the two types of rotation. The results are shown in Fig. 2. As mentioned above, in the two cases, the critical rotational frequencies for creating one vortex are very similar. As the vortex number increases, the two corresponding critical rotational frequencies become increasingly different. For example, to create 12 vortices, the critical rotational frequency for the synthetic field is about twice that for the rotating frame.

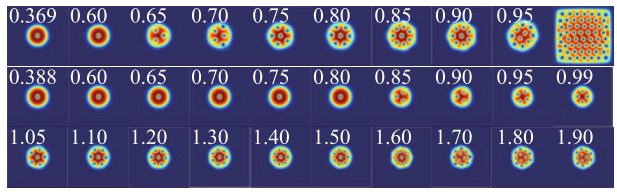


**Fig. 1** Contour plots of the density distributions $|\psi_{2\mathrm{D}}|^2$ showing a steady vortex state in a rotating BECs with the dimensionless contact interaction $g_{2\mathrm{D}} = 100$. Upper panels correspond to rotating frame. The middle (lower) panels correspond to synthetic magnetic field. The number in the panels shows the rotational frequency in units of $\omega_0$. The last figure in the upper panels corresponds to rotational frequency $0.99\omega_0$. The field of view in the panels is $8a_0 \times 8a_0$.

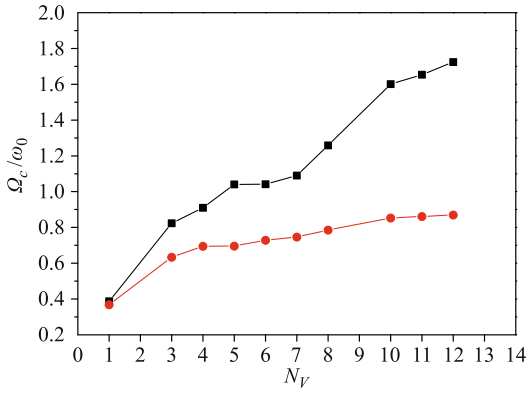


**Fig. 2** Plot of the equilibrium vortex number $N_V$ and rotational frequency of creating certain number vortices $\Omega_c/\omega_0$ for conventional BECs with the dimensionless contact interaction $g_{2D} = 100$. The square points and circle points are numerical results. The black and red lines represent synthetic magnetic field and rotating frame, respectively.

Note that the vortices are admitted into the condensate via dynamical instability [30, 21], and if the dynamical process of seeding vortices inside the condensate is taken into account, the critical rotational frequency should be larger than the value obtained using the present GP equation approach. Nevertheless, as shown by the analysis above, our treatment can provide a qualitatively reasonable description of the vortex formation process.

The Feynman rule for atomic BECs in a rotating trap has been studied [10, 15–18]. To proceed, we assess the validity of the Feynman rule for BECs in the synthetic magnetic field. Figure 3 shows the dependence of the vortex number $N_V$ and the angular momentum per atom $\ell_z/\hbar$ on the rotational frequency $\Omega/\omega_0$. The number $N_V$ is obtained from the density distribution, and the angular momentum per atom is numerically calculated according to the equation $\ell_z = \iint \psi^* L_z \psi \mathrm{d}x\mathrm{d}y / \iint |\psi|^2 \mathrm{d}x\mathrm{d}y$, where $L_z = -\mathrm{i}\hbar\,(x\partial_y - y\partial_x)$ is the $z$ component of the angular momentum operator. Numerical results show that the angular momentum per atom, $\ell_z/\hbar$, is about half of the number of vortices, so the Feynman rule basically holds for the two frames. The small disagreement between $N_V$ and $\ell_z/\hbar$ may be attributed to the inhomogeneous density [15].

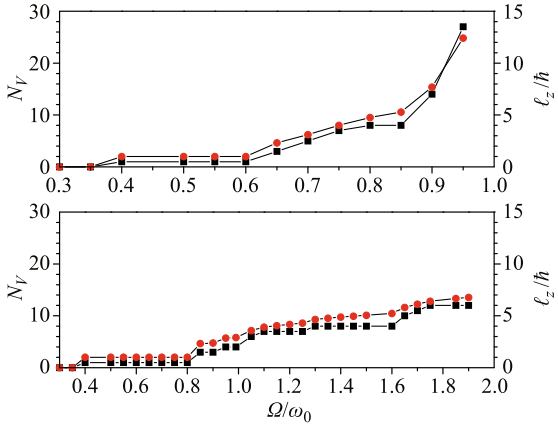


**Fig. 3** The number of vortices $N_V$ (black square points) and angular momentum per atom $\ell_z/\hbar$ (red circle points) versus rotational frequency $\Omega/\omega_0$ for conventional BECs with the dimensionless contact interaction $g_{2D} = 100$. The upper and lower panels correspond to rotating frame and synthetic magnetic field, respectively.

### 3.2 Effect of the contact interaction on vortex formation

According to the investigation of BECs in a rotating frame, interaction between atoms can affect the formation of vortices considerably [31]. Vortices can be created more easily in BECs with stronger repulsive interactions. It is of interest to study the role of contact interaction for BECs in a synthetic field. Figure 4 plots the critical rotational frequency $\Omega_{c1}/\omega_0$ for the single-vortex state as a function of the dimensionless contact interaction $g_{2D}$. The lower critical rotational frequency decreases monotonically with the contact interaction for both types of rotation, which indicates that the interaction has a similar effect on vortex formation in BECs rotated by the synthetic magnetic field.

Figure 5 illustrates the vortex structures at different values of $g_{2D}$. The rotational frequency is relatively large, $\Omega = 0.7\omega_0$. The upper and lower panels show the atom density for the rotating frame and synthetic field cases, respectively. By simply counting, we find that the ratios of the vortex numbers in the two cases are 5/1, 16/9, 24/17, 39/28, and 46/39 at $g_{2D} = 100$, 500, 1000, 2000, and 3000, respectively. For both cases, the vortex number increases with increasing interaction, and the ratio decreases and tends to unity. These results suggest that

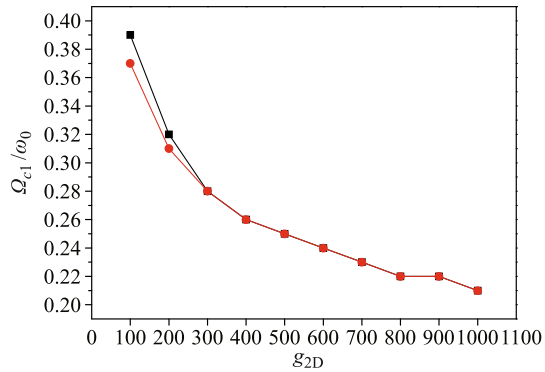


**Fig. 4** The lower critical rotational frequency $\Omega_{c1}/\omega_0$ for the single-vortex state as a function of the dimensionless contact interaction $g_{2D}$. The square points and circle points are numerical results. The black and red lines represent synthetic magnetic field and rotating frame, respectively.

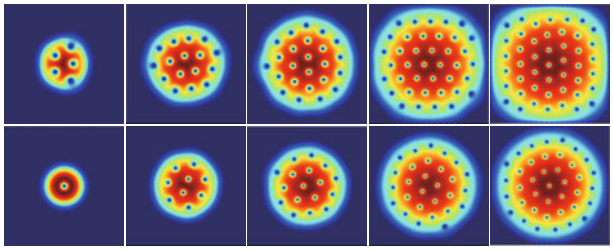

**Fig. 5** Upper and lower panels: density profiles for rotating frame and synthetic magnetic field at $\Omega = 0.7\omega_0$. From left to right, the dimensionless contact interaction is 100, 500, 1000, 2000, and 3000, respectively. The field of view in the panels is $8a_0 \times 8a_0$.

although it is still relatively difficult to generate vortices in the latter case compared to the former one, the difference between the two cases becomes small at sufficiently large contact interactions. For example, the vortex numbers are comparable at $g_{2D} = 3000$, and lattice-like structures are formed in both cases. The vortex lattice has not been observed experimentally using the latter approach [20]. In atomic gases, the s-wave scattering length can be tuned easily via the Feshbach resonance [32, 33]. Thus, increasing the contact interaction is an effective and realizable route to adding more angular momentum and generating more vortices in condensates rotated by a synthetic magnetic field.

As shown in Fig. 5, the condensate apparently becomes larger as the interaction strengthens. It appears that it is easier to add vortices in a larger condensate when the particle number remains constant. This suggests a possible reason that it is easy to produce more vortices in BECs spun up by the rotating trap than in those spun up by the synthetic magnetic field: confinement of the trap potential. According to Eqs. (4) and (6), in the rotating frame, the effective trapping potential is weakened with the rotational frequency $\Omega$; thus, the condensate expands. Nevertheless, in the synthetic magnetic field case, the trapping potential is independent of the Larmor frequency.

Finally, we briefly discuss the effect of the trap aspect ratio, $\gamma_z = \omega_z/\omega_0$, on vortex formation. This issue has been discussed for three-dimensional (3D) condensates in the rotating frame, and it is indicated that increasing $\gamma_z$ facilitates nucleation of the vortex [34]. In this study, the 3D system is converted into an effective 2D model, and the trap aspect ratio $\gamma_z$ is included in the effective 2D contact interaction $g_{2D} = \beta\sqrt{\gamma_z/2\pi}$, so the effect of increasing $\gamma_z$ is similar to that of increasing $g_{2D}$, as shown in Fig. 5.

## 4 Summary

We investigated the rotational properties of BECs in a synthetic magnetic field. Vortex formation was calculated by numerically solving the GP equation considering the effects of the Larmor (rotational) frequency, the interaction between atoms, and the trap aspect ratio. The obtained results were compared with those for BECs in a rotating frame. We found that the vortex number in the condensate spun up by the synthetic magnetic field is much smaller than that in the rotating frame given the same rotational frequency, which implies that the synthetic magnetic field rotates the condensate less efficiently. Strengthening the repulsive interaction between atoms or increasing the trap aspect ratio are helpful for creating more vortices. In particular, when the interaction is sufficiently strong, comparable large numbers of vortices are produced by both types of rotation. Abrikosov-lattice-like structures can be formed in both cases. Moreover, the validity of the Feynman rule was verified for BECs in the synthetic magnetic field.

**Acknowledgements** The authors are grateful to Weizhu Bao for valuable assistance in the numerical and programming techniques. This work was supported by the National Key Basic Research Program of China (Grant No. 2013CB922002), the National Natural Science Foundation of China (Grant No. 11074021), and the Fundamental Research Funds for the Central Universities of China.

## References

1. R. J. Donnelly, Quantum Vortices in Helium II, Cambridge: Cambridge University Press, 1991
2. D. Vollhardt and P. Wölfle, The Superfluid Phases of Helium 3, London: Taylor & Francis, 1990
3. G. E. Volovik, The Universe in a Helium Droplet, Oxford: Clarendon, 2003
4. G. Blatter, M. V. Feigel'man, V. B. Geshkenbein, A. I. Larkin, and V. M. Vinokur, Vortices in high-temperature superconductors, *Rev. Mod. Phys.* 66(4), 1125 (1994)
5. A. L. Fetter, Rotating trapped Bose–Einstein condensates, *Rev. Mod. Phys.* 81(2), 647 (2009)
6. M. R. Matthews, B. P. Anderson, P. C. Haljan, D. S. Hall, C. E. Wieman, and E. A. Cornell, Vortices in a Bose–Einstein condensate, *Phys. Rev. Lett.* 83(13), 2498 (1999)
7. K. W. Madison, F. Chevy, W. Wohlleben, and J. Dalibard, Vortex formation in a stirred Bose–Einstein condensate, *Phys. Rev. Lett.* 84(5), 806 (2000)
8. F. Chevy, K. W. Madison, and J. Dalibard, Measurement of the angular momentum of a rotating Bose–Einstein condensate, *Phys. Rev. Lett.* 85(11), 2223 (2000)
9. C. Raman, J. R. Abo-Shaer, J. M. Vogels, K. Xu, and W. Ketterle, Vortex nucleation in a stirred Bose–Einstein condensate, *Phys. Rev. Lett.* 87(21), 210402 (2001)
10. J. R. Abo-Shaeer, C. Raman, J. M. Vogels, and W. Ketterle, Observation of vortex lattices in Bose–Einstein condensates,

*Science* 292(5516), 476 (2001)

11. S.-W. Song, L. Wen, C.-F. Liu, S.-C. Gou, and W.-M. Liu, Ground states, solitons and spin textures in spin-1 Bose–Einstein condensates, *Front. Phys.* 8(3), 302 (2013)
12. V. Bretin, S. Stock, Y. Seurin, and J. Dalibard, Fast rotation of a Bose–Einstein condensate, *Phys. Rev. Lett.* 92(5), 050403 (2004)
13. V. Schweikhard, I. Coddington, P. Engels, V. P. Mogendorff, and E. A. Cornell, Rapidly rotating Bose–Einstein condensates in and near the lowest Landau level, *Phys. Rev. Lett.* 92(4), 040404 (2004)
14. R. P. Feynman, Application of Quantum Mechanics to Liquid Helium, Amsterdam: North-Holland, 1955
15. M. Tsubota, K. Kasamatsu, and M. Ueda, Vortex lattice formation in a rotating Bose–Einstein condensate, *Phys. Rev. A* 65(2), 023603 (2002)
16. K. Kasamatsu, M. Tsubota, and M. Ueda, Nonlinear dynamics of vortex lattice formation in a rotating Bose–Einstein condensate, *Phys. Rev. A* 67(3), 033610 (2003)
17. D. L. Feder and C. W. Clark, Superfluid-to-solid crossover in a rotating Bose–Einstein condensate, *Phys. Rev. Lett.* 87(19), 190401 (2001)
18. P. C. Haljan, I. Coddington, P. Engels, and E. A. Cornell, Driving Bose–Einstein-condensate vorticity with a rotating normal cloud, *Phys. Rev. Lett.* 87(21), 210403 (2001)
19. Y.-J. Lin, R. L. Compton, A. R. Perry, W. D. Phillips, J. V. Porto, and I. B. Spielman, Bose–Einstein condensate in a uniform light-induced vector potential, *Phys. Rev. Lett.* 102(13), 130401 (2009)
20. Y.-J. Lin, R. L. Compton, K. Jiménez-García, J. V. Porto, and I. B. Spielman, Synthetic magnetic fields for ultracold neutral atoms, *Nature* 462(7273), 628 (2009)
21. L. B. Taylor, R. M. W. van Bijnen, D. H. J. O'Dell, N. G. Parker, S. J. J. M. F. Kokkelmans, and A. M. Martin, Synthetic magnetohydrodynamics in Bose–Einstein condensates and routes to vortex nucleation, *Phys. Rev. A* 84(2), 021604(R) (2011)
22. M. Aidelsburger, M. Atala, S. Nascimbène, S. Trotzky, Y.-A. Chen, and I. Bloch, Experimental realization of strong effective magnetic fields in an optical lattice, *Phys . Rev. Lett.* 107(25), 255301 (2011)
23. Y. Nakano, K. Kasamatsu, and T. Matsui, Finite-temperature phase structures of hard-core bosons in an optical lattice with an effective magnetic field, *Phys. Rev. A* 85(2), 023622 (2012)
24. J. Xu and Q. Gu, Berezinskii–Kosterlitz–Thouless transition of two-dimensional Bose gases in a synthetic magnetic field, *Phys. Rev. A* 85(4), 043608 (2012)
25. A. Celi, P. Massignan, J. Ruseckas, N. Goldman, I. B. Spielman, G. Juzeliūnas, and M. Lewenstein, Synthetic gauge fields in synthetic dimensions, *Phys. Rev. Lett.* 112(4), 043001 (2014)
26. C. E. Creffield and F. Sols, Generation of uniform synthetic magnetic fields by split driving of an optical lattice, *Phys. Rev. A* 90(2), 023636 (2014)
27. J.-H. Fan, Q. Gu, and W. Guo, Thermodynamics of charged ideal Bose gases in a trap under a magnetic field, *Chin. Phys. Lett.* 28(6), 060306 (2011)
28. Y. Li and Q. Gu, Thermodynamic properties of rotating trapped ideal Bose gases, *Phys. Lett. A* 378(18–19), 1233 (2014)
29. W. Bao, I.-L. Chern, and F. Y. Lim, Efficient and spectrally accurate numerical methods for computing ground and first excited states in Bose–Einstein condensates, *J. Comp. Phys.* 219(2), 836 (2006)
30. S. Sinha and Y. Castin, Dynamic Instability of a rotating Bose–Einstein condensate, *Phys. Rev. Lett.* 87(19), 190402 (2001)
31. Y. Zhao, J. An, and C.-D. Gong, Vortex competition in a rotating two-component dipolar Bose–Einstein condensate, *Phys. Rev. A* 87(1), 013605 (2013)
32. G. Thalhammer, G. Barontini, L. De Sarlo, J. Catani, F. Minardi, and M. Inguscio, Double species Bose–Einstein condensate with tunable interspecies interactions, *Phys. Rev. Lett.* 100(21), 210402 (2008)
33. C. Chin, R. Grimm, P. Julienne, and E. Tiesinga, Feshbach resonances in ultracold gases, *Rev. Mod. Phys.* 82(2), 1225 (2010)
34. L. Santos, G. V. Shlyapnikov, P. Zoller, and M. Lewenstein, Bose–Einstein condensation in trapped dipolar gases, *Phys. Rev. Lett.* 85(9), 1791 (2000)